Hindawi
Mathematical Problems in Engineering
Volume 2018, Article ID 5153292, 12 pages
https://doi.org/10.1155/2018/5153292

Research Article

Modeling and Analysis of Effective Case Depth on Meshing Strength of Internal Gear Transmissions

Dezheng Liu,[1] **Yan Li**,[1] **Zhongren Wang**,[1] **You Wang**,[1] **and Yu Wang**[2]

[1]*Department of Mechanical Engineering, Hubei University of Arts and Science, Xiangyang, Hubei 441053, China*
[2]*Shanghai Institute of Applied Physics, Chinese Academy of Sciences, Shanghai 201800, China*

Correspondence should be addressed to Zhongren Wang; wzrvision@hbuas.edu.cn

Received 18 July 2018; Revised 27 November 2018; Accepted 17 December 2018; Published 30 December 2018

Guest Editor: Yingyot Aue-u-lan

The effective case depth (ECD) plays an important role in the meshing strength of internal gear transmissions. Carburizing quenching heat treatment is commonly used to enhance gear strength and wear resistance. However, the different ECDs in internal and external gears caused by heat treatment significantly affect the meshing strength, causing vibration, reducing gear service life, and hastening malfunction in internal gear transmission. In this study, we conducted an investigation of different ECDs by the heat treatment of carburized gear pairs by numerical simulation with the finite element method (FEM) and experiment tests. We analyzed three different carburized layer models, with the ECD in the internal gear being greater than, less than, and equal to the ECD in the external gear. In addition, we investigated the ability to distinguish between hardness gradients in gear teeth by dividing the carburized depth into seven layers to improve modeling accuracy. Results revealed that the meshing strength of internal gear transmission could be significantly enhanced by adopting the model with the ECD in the internal gear being less than the ECD in the external gear, and moreover, the shear stress of carburized gears initially increased and then decreased along with depth direction, and the maximum value appeared in the middle of the lower surface.

1. Introduction

With the overall development of science and technology, gear transmission has been progressively developed toward light weight, high load capacity, and low energy consumption. Carburizing and quenching heat treatment have been widely adopted to enhance gear strength and wear resistance. The use of a carburizing process in gear transmission systems is an important means of achieving a lightweight gear design because the carburized gear teeth usually acquire sufficient toughness, hardness, and wear resistance [1, 2]. It is well known that the increase of carburizing depth can improve the strength of gears and prevent failure. However, the increases in production and energy consumption may result from carburizing depths that are too large, which may lead to high-difficulty processes and the growth of the process cycle. ECD is closely related to the meshing strength and reliability of gears; thus, the design of an optimum ECD can not only improve the strength of gears but also avoid high cost and wasted energy.

Most current studies on carburized gears are limited to the theory of carburizing and quenching heat treatment and strength analysis for fatigue failure and rarely involve the accurate modeling and analysis of the effects of ECD on meshing strength of internal gear transmission. The distribution of hardness and shear stress under the tooth surface is closely related to the failure of internal gear transmission and thus has attracted significant attention from many researchers studying the evolution of shear stress in meshing gears. Li *et al.* [3] investigated different forms of failure of carburized gears using finite element (FE) simulation analysis by ANSYS; however, Li *et al.* [4] demonstrated that the modeling process and performance analysis of carburized gears were not detailed. Jiang [5] proposed a calculation method for maximum shear stress of gear contact surfaces and demonstrated that the most sensitive parameter of the largest stress is the maximum Hertz stress. Chen and Shao [6] proposed the mesh stiffness calculation method of external spur gear pairs based on applying the potential energy theory to the calculation of internal gear tooth deformation. Tang

and Liu [7] proposed a new simulation method and built a loaded multitooth contact model to investigate the contact stress of face-gear drives, proving that the adoption of the FEM in analyzing contact stress of face-gear drives is reliable. Nevertheless, these methods cannot meet the requirement of comprehensive analysis of carburized gear strength.

The hardness and elastic modulus at each point on and inside the gear surface are different after carburization, such that a carburized gear can be regarded as a heterogeneous material [8, 9]. Thus, the strengths and shear stresses at different ECDs are nonlinear in gear meshing. Kim and Bae [10] studied gear deformation at different quenching temperatures during carburizing-quenching simulation and proposed process parameters for practical manufacturing. Sugimoto [11] investigated the distortion in axial contraction of a carburized-quenched helical gear. Rajesh *et al.* [12] analyzed load sharing and bending strength for altered tooth-sum gears in which the tooth-profile shift greatly affected performance. In these studies, however, the strength and failure analysis based on experimental testing was discussed, and the related processes are usually expensive and time-consuming. Kim *et al.* [10] and Nojima *et al.* [13] proposed calculation methods for the ECD of carburized gears that, while involving only a few process parameters, did not analyze the strength of carburized gears.

From the publicly available literature, it is evident that work on the effects of ECD on meshing strength is limited, especially regarding internal gear transmission. Actually, the ECD has a great impact on the meshing strength, including not only the shear stress distribution but also the wear resistance, thus resulting in the possibility of meshing performance variation of the internal gear transmission [14, 15]. In this paper, we established an analytical calculation model for meshing shear stresses of an internal gear pair with a shifted tooth profile based on previous work [4, 16, 17] with consideration for the friction factor. The proposed model made it possible to reveal the effect of ECD on the meshing strength of an internal gear pair via the different ECDs achieved by heat treatment of a carburized gear pair made of 805M20 steel through numerical simulation using FEM and experiment. We analyzed three different carburized layer models, with the ECD of an internal gear being greater than, less than, and equal to the ECD in an external gear. We realized the distinguishing of hardness gradients in gear teeth by dividing the ECD into seven layers to improve the analysis accuracy.

This paper is organized as follows. Reviews of the previous literature on gear ECD and the meshing strength calculation method were presented previously. Thus, in Section 2, an analytical meshing formulation of a carburized gear pair is derived, followed by the construction of an internal gear transmission model. The results and discussion of the investigation of the effect of ECD on the meshing strength of internal gear transmissions are presented in Section 3. Conclusions are drawn in Section 4.

2. Materials and Methods

2.1. Analytical Meshing Formulation of Carburized Gear. The meshing strength performance of a gear is determined by the shear strength of the gear material and shear stress distribution under the tooth surface [18]. Reasonable selection of the depth of the carburizing layer can improve the strength and the rolling contact durability of powder metallurgical gears. The radius of curvature of the involute surface of the gear can be regarded as the radius of the cylinder when a pair of involute gears is engaged. Therefore, the contact problem of the two meshing teeth can be simplified as the contact problem of two cylinders. The meshing-tooth model is illustrated in Figure 1(a) and the stress state under the contact surface is shown in Figure 1(b), in which the vertical direction of the contact surface is the Z axis and the horizontal direction is the Y axis. The contact surface is affected by the normal load P, and the friction between the two contact surfaces is q.

The maximum contact stress $P_{\max}$ and the half-width of Hertz contact zone b can be expressed as follows:

$$P_{\max} = \sqrt{\frac{W}{\pi} \cdot \frac{(R_1 + R_2)/R_1R_2}{[(1-\nu_1^2)/E_1 + (1-\nu_2^2)/E_2]}} \tag{1}$$

$$b = \sqrt{\frac{4W}{\pi} \cdot \frac{R_1R_2}{R_1 + R_2}\left[\frac{1-\nu_1^2}{E_1} + \frac{1-\nu_2^2}{E_2}\right]} \tag{2}$$

where W is the load per unit length of gear teeth, R_1 and R_2 are the curvature radii at the contact point, E_1 and E_2 are Young's moduli, and ν_1 and ν_2 are Poisson's ratios.

In gear meshing, the carburized layer involves alternating shear stress. Spalling will occur when the shear stress exceeds the ultimate strength of the material [19]. By ignoring the friction, the stress at an arbitrary point under the gear surface can be calculated by the following formulas:

$$\sigma_{yy} = \frac{\left[\left(\sqrt{1 + (z/b)^2} - z/b\right)^2 / \sqrt{1 + (z/b)^2}\right] b}{\Delta} \tag{3}$$

$$\sigma_{zz} = -\frac{\left[1/\sqrt{1 + (z/b)^2}\right] b}{\Delta} \tag{4}$$

$$\sigma_{xx} = -\frac{2\nu\left[\sqrt{1 + (z/b)^2} - z/b\right] b}{\Delta} \tag{5}$$

$$\Delta = \frac{2}{1/R_1 + 1/R_2}\left[\frac{1-{\nu_1}^2}{E_1} + \frac{1-{\nu_2}^2}{E_2}\right] \tag{6}$$

where b is the half-width of the Hertz contact zone and z the distance beneath the tooth surface. The maximum shear stress can be expressed as follows:

$$\tau_{\max} = \frac{1}{2}(\sigma_{\max} - \sigma_{\min}) \tag{7}$$

$\sigma_{\max}$ takes the maximum value of σ_{xx}, σ_{yy}, and σ_{zz}, and $\sigma_{\min}$ takes the minimum value of σ_{xx}, σ_{yy}, and σ_{zz}.

In practical engineering application, the calculation of gear-meshing strength analytically always can be achieved by considering the friction influence. In addition to the panel

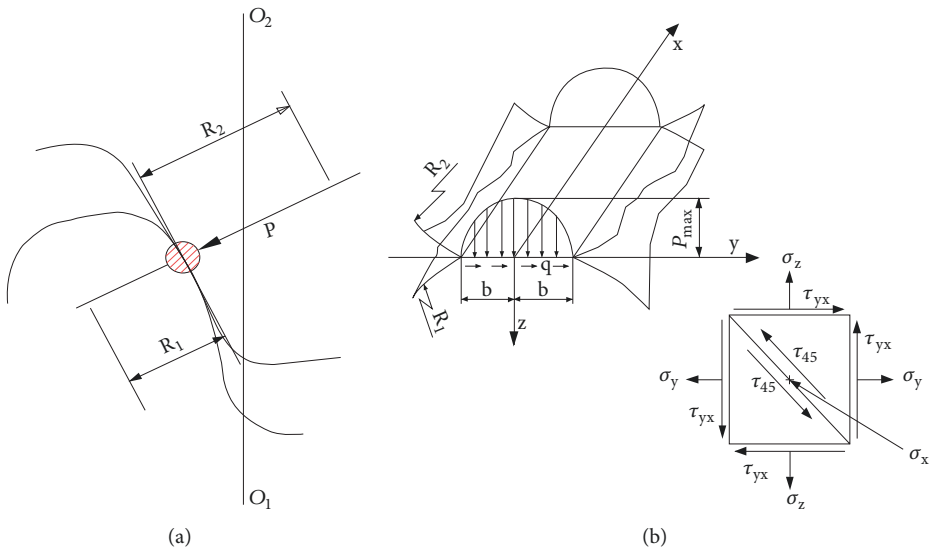

(a) (b)

Figure 1: Stress state under the contact surface of gear teeth: (a) involute gear meshing and (b) stress distribution on gear surface.

node, the rest of the meshing points experience both rolling and sliding. Therefore, the contact area simultaneously bears the normal force and tangential force [20]. According to Hertz theory [21], the stress at an arbitrary point under the combined effect of normal pressure and shear stress can be calculated by the following formulas:

$$\sigma_{yy} = -\frac{b}{\pi\Delta}\left\{z\left(\frac{b^2+2z^2+2y^2}{b}\Phi_1 - \frac{2\pi}{b} - 3y\Phi_2\right) + f\left[\left(2y^2-2b^2-3z^2\right)\Phi_2 + \frac{2\pi y}{b} + 2\left(b^2-x^2-z^2\right)\frac{y}{b}\Phi_1\right]\right\} \tag{8}$$

$$\sigma_{xx} = -\frac{2vb}{\pi\Delta}\left\{z\left(\frac{b^2+z^2+y^2}{b}\Phi_1 - \frac{\pi}{b} - 2y\Phi_2\right) + f\left[\left(y^2-b^2-z^2\right)\Phi_2 + \frac{\pi y}{b} + \left(b^2-x^2-z^2\right)\frac{y}{b}\Phi_1\right]\right\} \tag{9}$$

$$\sigma_{zz} = -\frac{b}{\pi\Delta}\left[z\left(b\Phi_1 - y\Phi_2\right) + {f_z}^2\Phi_2\right] \tag{10}$$

$$\tau_{yz} = -\frac{b}{\pi\Delta}\left\{z^2\Phi_2 + f\left[\left(c^2+2y^2+2z^2\right)\frac{z}{b}\Phi_1 - \frac{2\pi z}{b} - 3yz\Phi_2\right]\right\} \tag{11}$$

where f is the friction coefficient and v Poisson's ratio:

$$\Phi_1 = \frac{\pi(M+N)}{MN\sqrt{2MN+2y^2+2z^2-2b^2}} \tag{12}$$

$$\Phi_2 = \frac{\pi(M-N)}{MN\sqrt{2MN+2y^2+2z^2-2b^2}} \tag{13}$$

$$M = \sqrt{(b+y)^2+z^2} \tag{14}$$

$$N = \sqrt{(b-y)^2+z^2} \tag{15}$$

The formulas for the three principal stresses can be expressed as follows:

$$\sigma_1 = \frac{\sigma_{yy}+\sigma_{zz}}{2} + \sqrt{\left(\frac{\sigma_{yy}-\sigma_{zz}}{2}\right)^2 + {\tau_{yz}}^2} \tag{16}$$

$$\sigma_2 = v\left(\sigma_{yy}+\sigma_{zz}\right) \tag{17}$$

$$\sigma_3 = \frac{\sigma_{yy}+\sigma_{zz}}{2} - \sqrt{\left(\frac{\sigma_{yy}-\sigma_{zz}}{2}\right)^2 + {\tau_{yz}}^2} \tag{18}$$

According to the third strength theory, the maximum shear stress value on the principal shear stress plane can be expressed as follows:

$$\tau_{\max} = \frac{1}{2}\left(\sigma_1 - \sigma_3\right) \tag{19}$$

where σ_1 and σ_3 are the maximum and minimum algebraic values of the principal stress, respectively. On the basis of the Tresca criterion [22], the relationship between the yield strength (YS) and the critical shear fracture stress has been described by Ashby and Jones [23]. The formula of the critical shear fracture stress can be written as follows:

$$2\tau_0 = 1.15\sigma_y \tag{20}$$

where τ_0 is the critical fracture stress in MPa and σ_y the yield stress in MPa.

The spalling failure of a gear is related to the loads, ECD, and hardness in the tooth heart [24]. Under certain assumptions concerning the loads, the crack that originates from the transition layer will cause deep spalling if the ECD is too shallow or the hardness in the tooth heart is low. When the hardness in the gear-tooth center meets the requirement of strength, the crack that originates from the hardness layer will cause shallow spalling if the defects exist in the structure of the hardness layer.

The junction between the hardness layer and tooth heart is a weak region [4]. To avoid spalling produced by the transition layer, it is essential to design a reasonable ECD. Ding and Rieger [25] indicated that the spalling failure of a gear is caused by orthonormal shear stress and proposed the conditions in which the hardness and transition layers do not produce spalling cracks:

$$A\left(\frac{\tau_{yz}}{\mathrm{HV}}\right)_t \le 0.6A\left(\frac{\tau_{yz}}{\mathrm{HV}}\right)_{\mathrm{lim}} \tag{21}$$

$$A\left(\frac{\tau_{yz}}{\mathrm{HV}}\right)_H \le 0.6A\left(\frac{\tau_{yz}}{\mathrm{HV}}\right)_{\mathrm{lim}} \tag{22}$$

where τ_{yz} is the orthonormal shear stress, $A(\tau_{yz}/\mathrm{HV})_t$ is the extreme value in the transition layer, $A(\tau_{yz}/\mathrm{HV})_H$ is the extreme value in the hardness layer, and $A(\tau_{yz}/\mathrm{HV})_{\mathrm{lim}}$ is the limit amplitude.

Some researchers [4, 26, 27] have indicated that the spalling failure of a gear is caused by the maximum shear stress and proposed that the ratio of the shear stress in the transition layer and the shear strength of the gear material should not be larger than 0.55, which is expressed as follows:

$$\varepsilon = \frac{\tau_{\max}}{[\tau]} \le 0.55 \tag{23}$$

where ε is the ratio of the shear stress in the transition layer and shear-strength resistance, $\tau_{\max}$ is the maximum shear stress, and $[\tau]$ is a material property of the shear strength for gear.

The depth of the hardness layer is an important technical index in the carburizing and quenching heat treatment of gears. Calculation of the depth of the hardness layer could be achieved analytically by regarding the gear teeth as nonuniform cantilever beams [28, 29], which has been employed in previously published papers to give the recommended value of the depth of the hardness layer to prevent spalling failure based on the maximum shear stress caused by gear meshing. The formula [30] for calculating the minimum depth of the hardness layer at the pitch circles of the gear tooth can be expressed as follows:

$$h_e = \frac{S_C \cdot d \cdot \sin\alpha}{U_H \cdot \cos\beta} \mathrm{C_G} \tag{24}$$

where h_e is the minimum depth of the hardness layer at the pitch circles, S_c is the contact stress, α is the pressure angle of the end surface of the pitch circle, d is the diameter of the pitch circle, β is the base helix angle, U_H is the hardening process coefficient, and C_G is the transmission ratio coefficient.

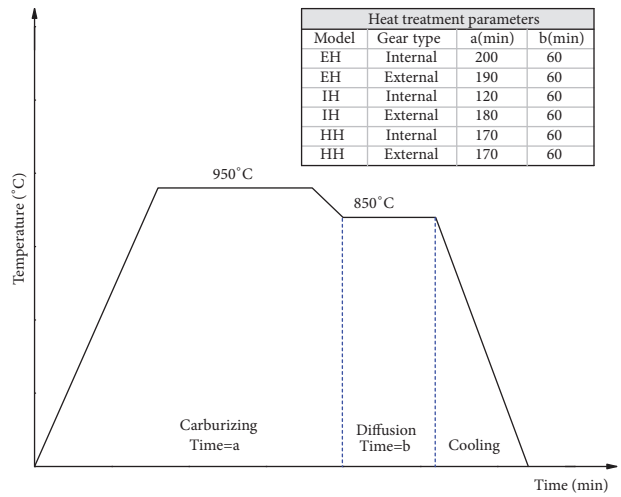

Figure 2: Process curve for heat treatment of gear.

More detailed expressions of the empirical formula [31] for the depth of the hardness layer at each meshing point of the tooth surface can be derived and expressed as follows:

$$t_i = 1.66 \times 10^3 \times \left(1 + \frac{w(C_i) - w(C_{\mathrm{inner}})}{w(C_{\mathrm{outer}}) - w(C_i)}\right) \times \left[\frac{T_1 \times z_2 \tan\alpha}{z_1 + z_2}\right]^{1/2} \tag{25}$$

where t_i is the thickness of each point of the carburized layer, $w(C_{\mathrm{outer}})$ is the carbon intensity of the gear surface, $w(C_{\mathrm{inner}})$ is the carbon intensity of the gear heart, $w(C_i)$ is the carbon intensity of each point of the carburized layer, T_1 is the torque of the driving gear, z_1 is the number of driving-gear teeth, and z_2 is the number of driven-gear teeth.

The empirical formula [31] for the calculation of the minimum depth of the carburized layer can be written as follows:

$$t \ge \frac{31a \times \sin\alpha_t \times \delta_{\max} \times u}{Hv \times \cos\beta_h \times (u \pm 1)^2} \tag{26}$$

where t is the minimum depth of the carburized layer, a is the center distance of the gear pair, a_t is the engaged angle of the gear transverse plane, $\delta_{\max}$ is the maximum contact stress, u is the gear transmission ratio, Hv is the Vickers hardness of the carburized layer of the gear surface in kg/mm^2, β_h is the base helix angle, and "+" and "−" represent external meshing and internal meshing, respectively.

2.2. Internal Gear Transmission Model. The complete die-quenching process for a gear pair includes carburizing, die quenching, and air cooling. The complete technical curve is shown in Figure 2. The gear pairs made of 805M20 steel were carburized in a double-ring hearth furnace consisting of carburizing and diffusion units. We applied load to the gear before the quenching process and removed load after the quenching process. To investigate the effects of ECD on the

Table 1: Parameters for external and internal gears.

Gear pair	Tooth number	Modulus (mm)	Tooth width (mm)	Pressure angle (°)	Pitch diameter (mm)
External gear	35	1.60	3.5	33.94	45.54
Internal gear	36	1.63	3.5	33.94	46.84

meshing strength of internal gear transmission, we devised three different carburized layer models, with the carburized-layer depth in the internal gear being greater than, less than, and equal to the carburized-layer depth in the external gear.

The hardness-gradient measurement was carried out by Vickers microhardness measurements after gear-tooth cutting. A 300-g load was used for the microhardness tests. The ECD was defined as the distance from the surface to the point at which the microhardness was 550 HV, and it was dependent on the carbon potential and the duration of the carburizing process [32]. The variation of hardness values with the carburized depth is shown in Figure 3. We built three mechanical models, (1) EH, (2) IH, and (3) HH, corresponding to the ECD in the internal gear being greater than, less than, and equal to the ECD in the external gear, in the static strength tests. The ECDs in the three mechanical models are shown in Figure 4.

Zhang *et al.* [22] described the physical relationship between hardness and strength and developed the correlations that allow for calculation of expected YSs from measured hardness. For a Vickers indenter, the relationship between hardness and strength through the pressure normal to the surface of the indenter tip can be calculated as follows:

$$\sigma_y = 3.12H_V, \tag{27}$$

$$\sigma_{UTS} = 3.26H_V, \tag{28}$$

where σ_y is the yield stress (YS) in MPa, H_V is the Vickers hardness of the carburized layer of the gear surface in kg/mm^2, and σ_{UTS} is the ultimate tensile strength (UTS) in MPa. In this study, we calculated the mechanical properties of three different carburized-layer models using (27) and (28); the relationship between strength and carburized-layer depth is plotted in Figure 5.

The parameters for external and internal gears are shown in Table 1. Under normal circumstances, gear failure usually occurs in the gear teeth and rarely in a part of the hub. To achieve high calculation accuracy, the hexahedron element is used in the mesh of the FEM model. We used a geometric model of the external and internal gears to represent the entire gear pair. There were 817906 nodes and 806721 elements in the FE mesh, as shown in Figure 6(a). We determined the hardness gradient in the gear teeth by dividing the carburized depth into seven layers, as shown in Figure 6(b).

We devised three different carburized-layer models, with the ECD in the internal gear being greater than, less than, and equal to the ECD in the external gear. In addition, we determined the hardness gradient in the gear teeth by dividing the carburized depth into seven layers to improve the modeling accuracy.

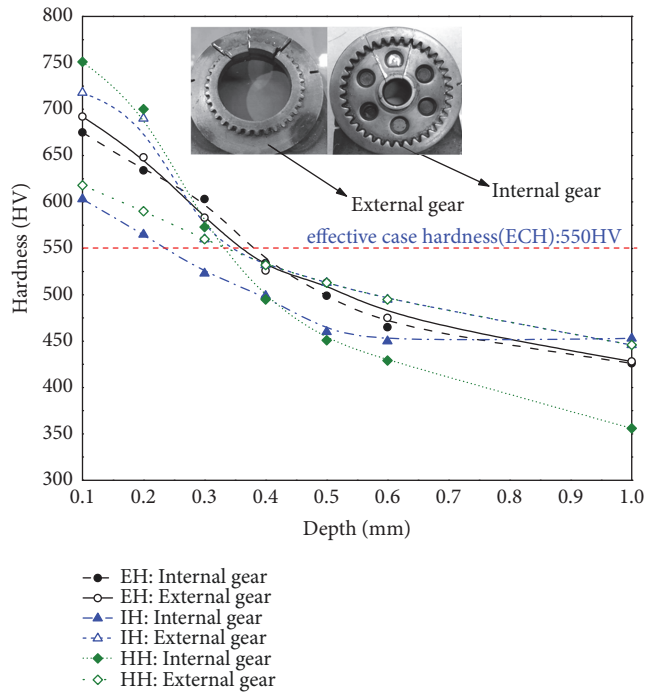

Figure 3: Variation of hardness value with carburized-layer depth.

3. Results and Discussion

In this study, we used three carburized gear-pair models (EH, IH, and HH models) for the static strength test. The external gear was fixed on a pedestal and the internal gear connected to a steel frame. The steel frame and a hydraulic drawing machine were connected flexibly through a steel cable; the piston of the hydraulic drawing machine was uniformly contracted in the cylinder, as shown in Figure 7. We recorded the displacement curve of the piston and the force of hydraulic cylinder to achieve the strength of carburized gear pair. The variation of maximum strength with gear rotation angle is shown in Figure 8.

The stress and displacement distribution of the carburized gear pair in any position can be achieved through transient analysis of the FEM models of the carburized gear pair using (1) to (19). The maximum stress can be obtained by reading the maximum contact stress on the surface of the tooth root of the carburized gear using (1). Furthermore, we calculated the maximum shear stress in the carburized layer

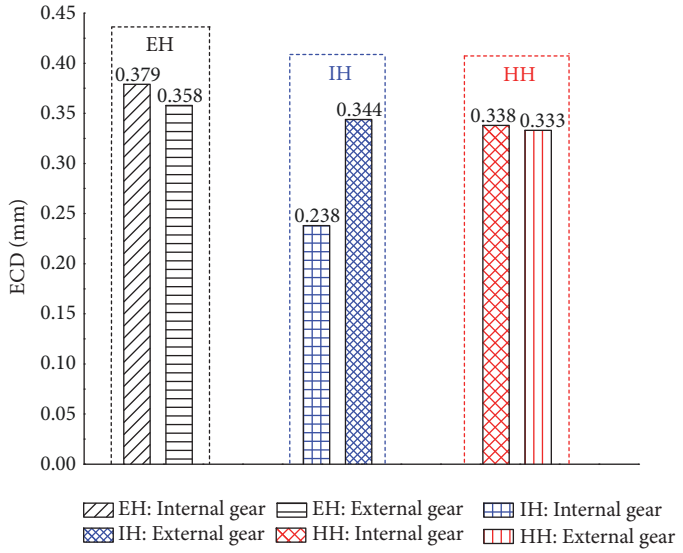

Figure 4: ECD in three mechanical models.

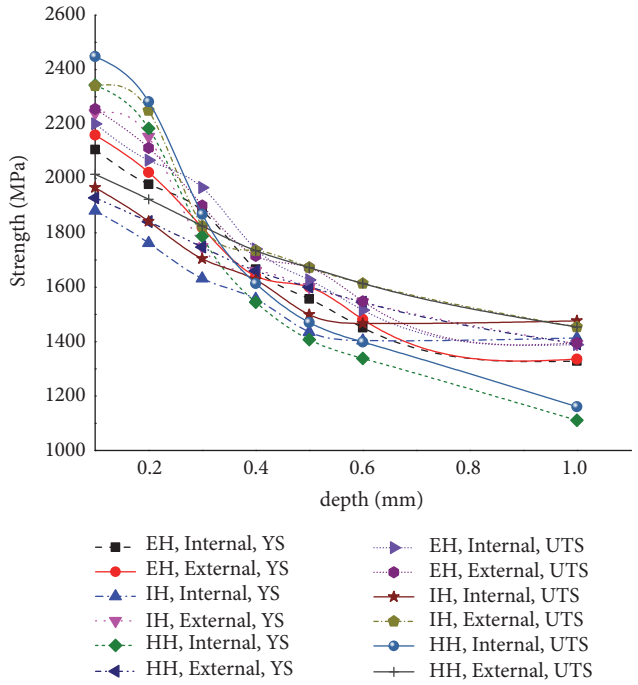

Figure 5: Relationship between strength and carburized-layer depth.

and obtained the worst meshing point and corresponding meshing-gear number. The maximum shear stress value and the maximum stress on the principal shear stress plane can be calculated by (7) and (19), respectively. The calculations were conducted through the use of the platform of ABAQUS software. The displacement distribution of the external gear teeth at the maximum meshing strength of three different gear pairs is shown in Figure 9.

The stress and displacement were zero at the beginning of engagement, but the stress increased significantly for the shock in the 24th pair of gear teeth and reduced with rotation. The maximum displacements in the EH, IH, and HH models were 1.594, 1.54, and 1.571 mm, respectively. The shear stress increased simultaneously upon engagement of a single tooth. Furthermore, the maximum shear stress was observed when the 24th pair of teeth meshed. By reading the maximum strength of the carburized gear-pair models, the variation of the maximum strength with gear rotation angle in the three models is shown in Figure 10.

According to Figure 10, the maximum strengths in the EH, IH, and HH models are 4322 N·m, 4609 N·m, and 4480 N·m, respectively. Thus, the highest strength of a carburized gear pair can be obtained when the carburized-layer depth in the internal gear is less than that in the external gear. The

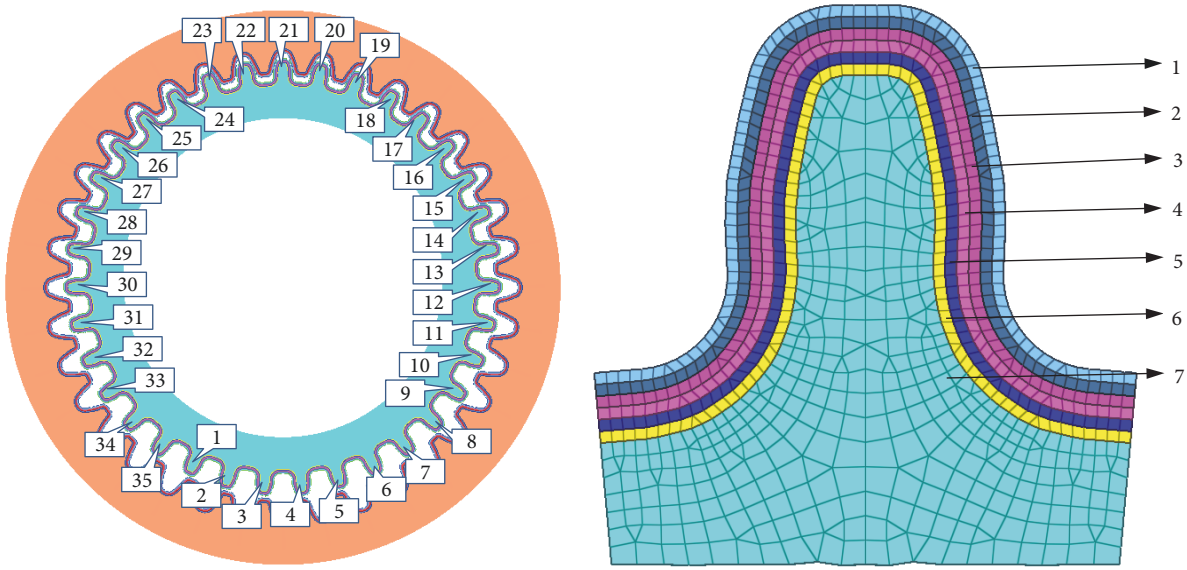

(a) (b)

Figure 6: Geometry and mesh of gear-pair model: (a) FE mesh model and (b) distinction of hardness gradient.

Figure 7: The loading apparatus for testing the maximum strength value of gear pairs.

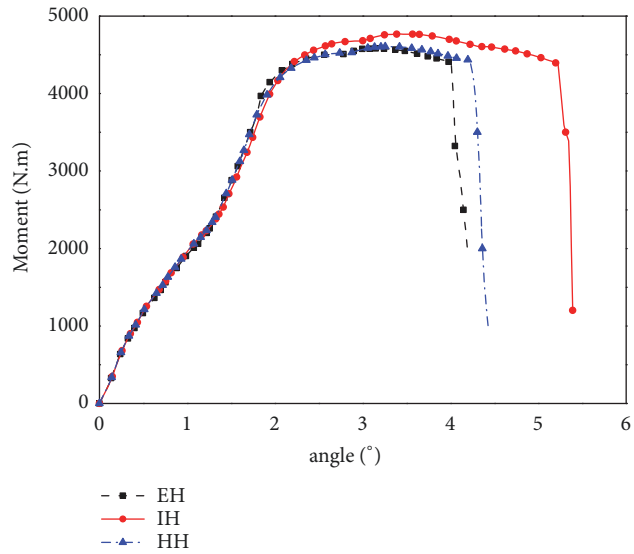

Figure 8: Variation of maximum strength with gear rotation angle based on experimental test.

maximum meshing strength predicted by the FEM is in good agreement with that determined from experiment. According to the von Mises criterion [33], the ductility of the different carburized gear pairs can be achieved based on the ability of the gear to absorb deformation energy before the failure of the gear pair; the deformation energies of the three gear-pair models studied before failure are shown in Figure 11.

In this study, we defined the ductility of different carburized gear pairs as the ratios of the total energy that the gear pairs can absorb before failure. For a volume of the gear pair of 3280 mm^3, we calculated the total energy by integration of the torque by rotation angle. The total deformation energies in different models are represented by the dashed area in Figure 12 and the strength and ductility of the three carburized gear-pair models studied are given in Table 2.

The strength and ductility of the IH gear-pair model are the highest of the three carburized gear-pair models studied. The results for the hardness gradients of the carburized gear pairs show that the meshing strength of internal gear transmission could be enhanced by adopting the IH gear-pair model with the ECD in the internal gear being less than the ECD in the external gear. The meshing strength performance of a gear is determined by the shear strength property of the gear material and shear stress distribution under the tooth surface. Selecting the IH gear-pair model, the shear stress and plastic strain of internal gear transmission are shown in Figure 12.

It can be seen from Figure 12 that the shear stress and plastic strain values for the external gear are obviously higher than those for the internal gear in gear engagement and

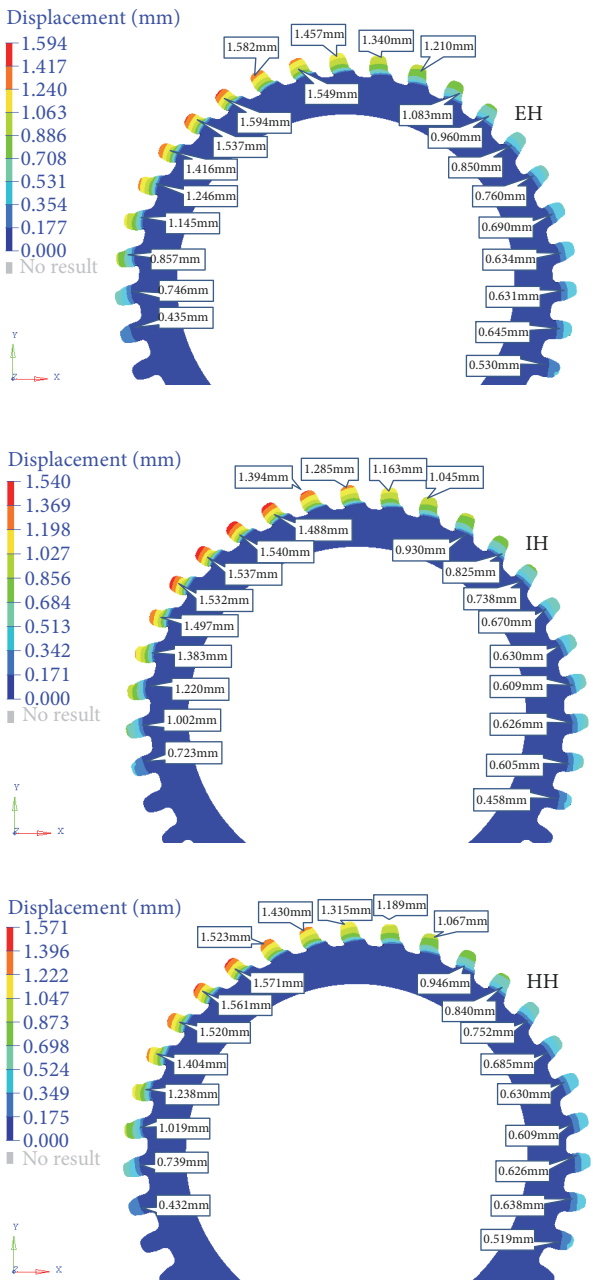

FIGURE 9: Displacement distribution of external gear teeth at maximum meshing strength of three different gear pairs.

the ECD in the internal gear has a limited influence on the strength and ductility of internal gear transmission. With an increasing number of engaged gears, the external gear will fail earlier than the internal gear.

On the basis of the Tresca criterion [22], we calculated the fracture stresses of the external gear in seven layers for the three mechanical models using (20) and the results are summarized in Table 3.

The strength of the IH gear-pair model is the highest of the three carburized gear-pair models. Using the maximum shear stress value, the maximum shear stress in each hardness layer for the external gear is presented in Figure 13.

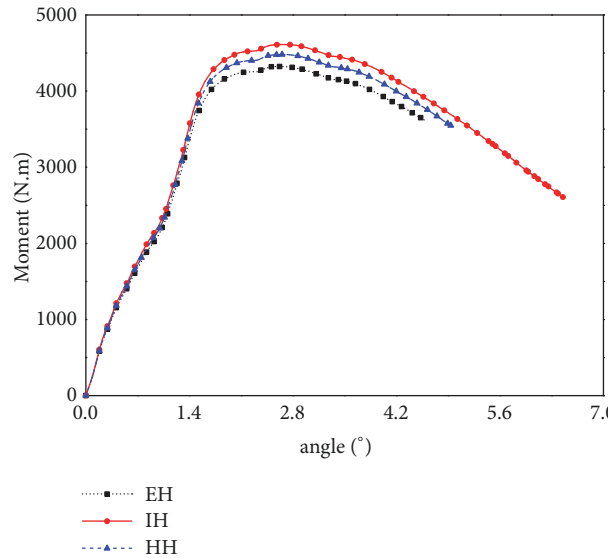

FIGURE 10: Variation of maximum strength with gear rotation angle based on FEM.

Figure 13 shows the maximum shear stress in each of seven hardness layers for the external gear and the speed sequence of the shear stress value in all seven layers that reaches the value of the fracture stress as follows: layer 4 > layer 3 > layer 7 > layer 5 > layer 6 > layer 2 > layer 1. Thus, the speed sequence of the shear stress value in all seven layers that reaches the value of the fracture stress indicates that the crack grows from the inside to the outside of the gear tooth. By selecting four points on the engaged tooth surface of the external gear in the IH model, the shear stresses on the engaged-tooth surface are shown in Figure 14.

Figure 14 shows the shear stresses on the engaged-tooth surface and that the growth sequence of the shear-stress value on the engaged tooth surface is P4 > P3 > P2 > P1, thus indicating that the crack grows from the middle to the sides of the gear-tooth surface.

4. Conclusions

We investigated the ECD of the internal carburized gear pairs using the FEM and experimental tests. We also analyzed three different carburized-layer models, with the ECD in the internal gear being greater than, less than, and equal to the ECD in the external gear. We derived the empirical formula for the calculation of the minimum depth of the carburized layer and then studied the specific process of establishing the FEM of a carburized gear pair. Finally, for the three carburized internal gear pairs studied, we performed numerical investigation of the meshing strength and compared the results with those of the experimental strength test. The following conclusions were drawn:

(1) The strength and ductility of the IH gear-pair model are the highest of the three carburized gear-pair models studied, and thus the ECD in the internal gear being less than the ECD in the external gear is the optimum configuration

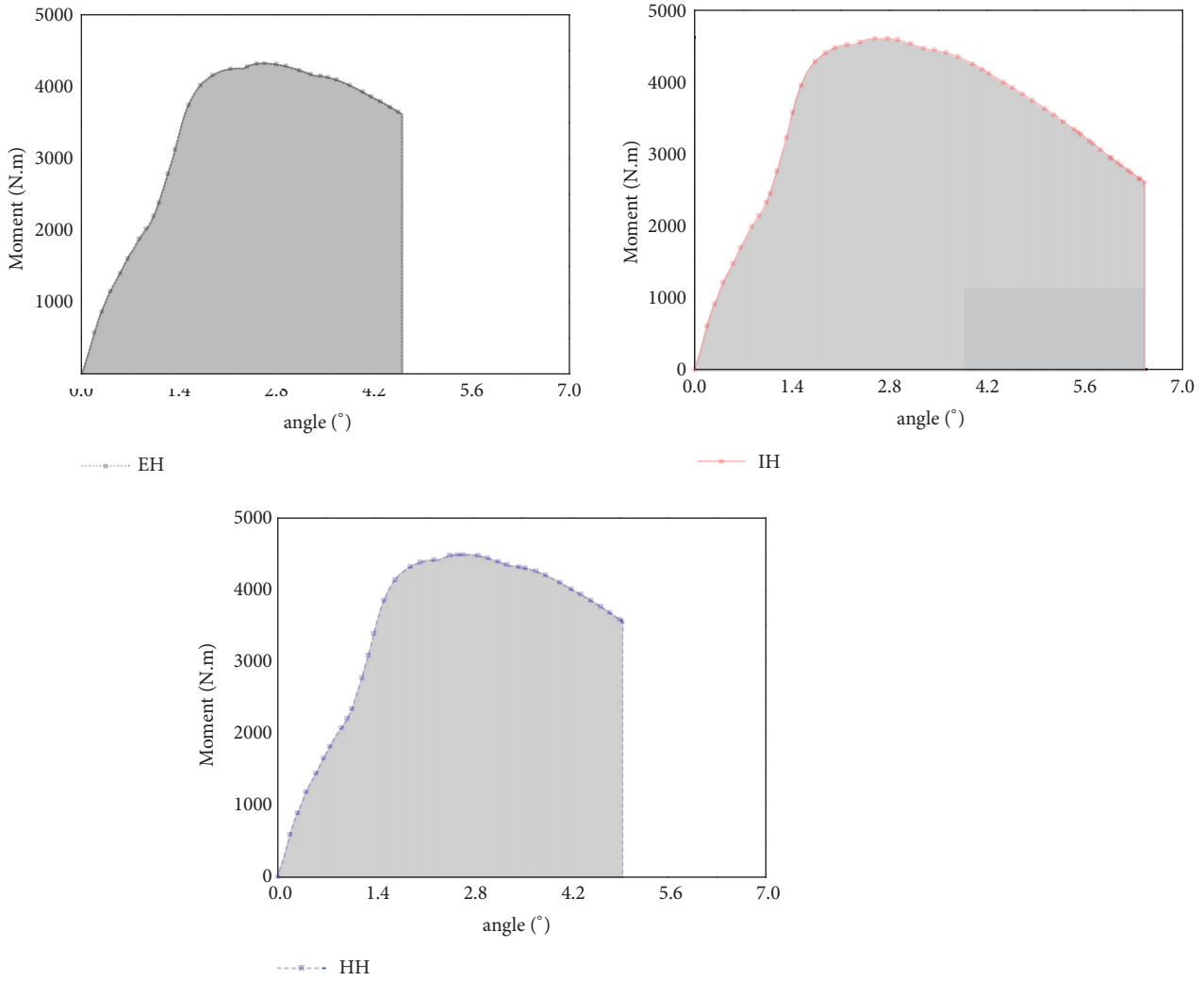

Figure 11: Deformation energies of three gear-pair models under study before failure.

Table 2: Strength and ductility of three carburized gear-pair models studied.

Carburized gear teeth	Gear-pair strength (N.m)	Strength ratio (based on EH model)	Gear-pair ductility (×100 kJ/mm^3)	Ductility ratio (based on EH model)
EH model	4322	1	814	1
IH model	4609	1.066	1195	1.468
HH model	4480	1.037	912	1.120

Table 3: Fracture stresses of external gears in seven layers for three mechanical models studied.

Layer number	Tresca criterion fracture stress (MPa)		
	EH	IH	HH
1	1241.448	1288.092	1108.692
2	1162.512	1237.86	1058.46
3	1045.902	1004.64	1004.64
4	943.644	954.408	954.408
5	920.322	920.322	920.322
6	852.15	888.03	888.03
7	767.832	800.124	800.124

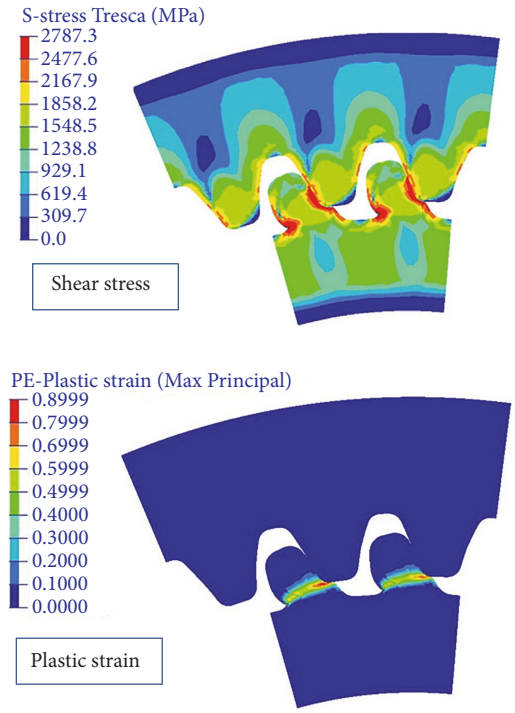

Figure 12: Shear stress and plastic strain of internal gear transmission.

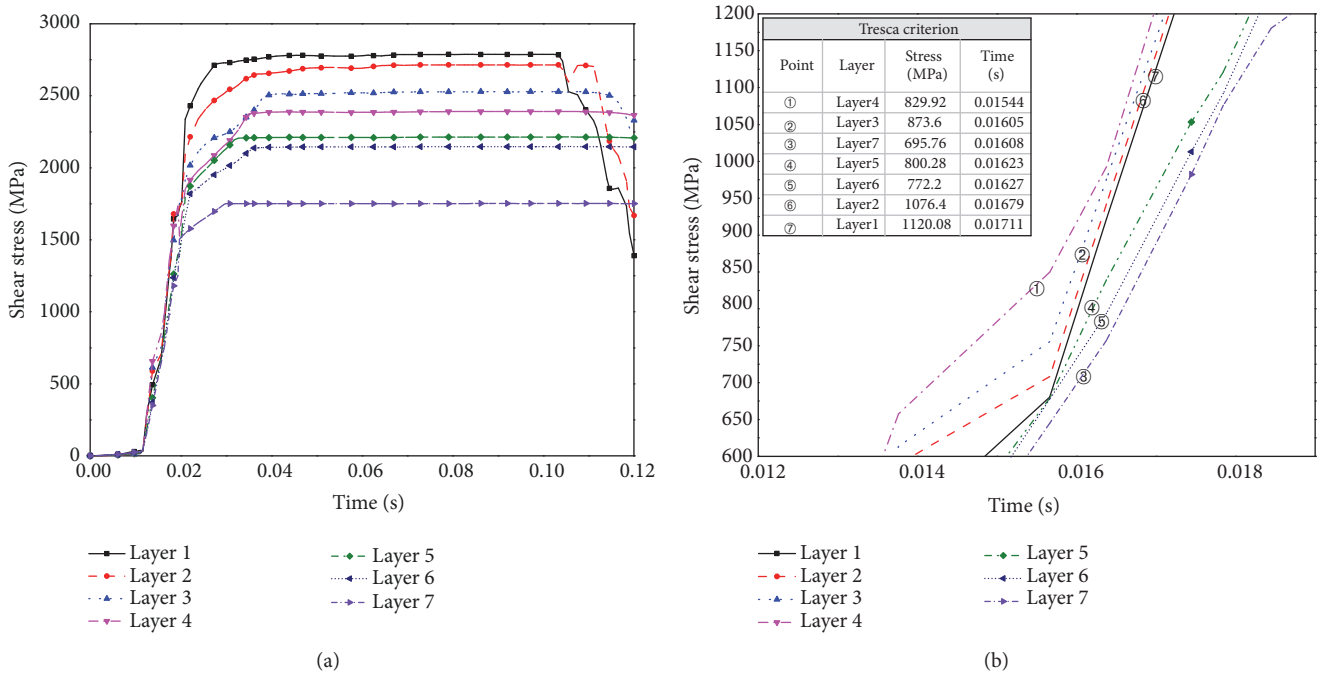

Figure 13: Maximum shear stress in each hardness layer for external gear: (a) evolution of maximum shear stress in seven layers; (b) sequence of shear stress in seven layers that reaches fracture stress from first to last.

in the design of the carburizing process for internal gear transmissions.

(2) The meshing strength of internal gear transmission is significantly affected by the shear strength of the gear material and shear stress distribution under the tooth surface; the shear stress of carburized gears initially increases and then decreases along with depth direction, and the maximum value appears in the middle of the lower surface.

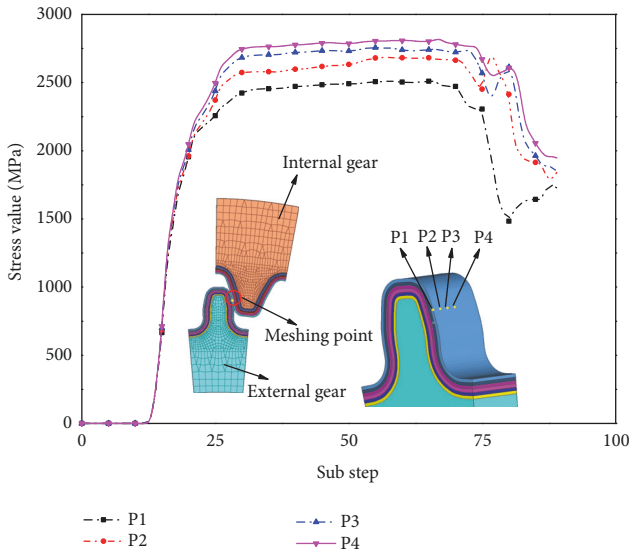

Figure 14: Shear stresses on engaged-tooth surface.

Data Availability

(1) The FE model catalysts data of the EH carburized gear-pair model used to support the findings of this study have been deposited in the FAIRsharing (https://fairsharing.org/) repository (DOI: https://doi.org/10.6084/m9.figshare.6875450.v1). (2) The FE model catalysts data of the HH carburized gear-pair model used to support the findings of this study have been deposited in the FAIRsharing (https://fairsharing.org/) repository (DOI: https://doi.org/10.6084/m9.figshare.6875456.v1). (3) The FE model catalysts data of the IH carburized gear-pair model used to support the findings of this study have been deposited in the FAIRsharing (https://fairsharing.org/) repository (DOI: https://doi.org/10.6084/m9.figshare.6875462.v1). (4) The experimental catalysts data of the hardness gradients of the three carburized gear-pair models used to support the findings of this study have been deposited in the FAIRsharing (https://fairsharing.org/repository) repository (DOI: https://doi.org/10.6084/m9.figshare.6875477.v1). (5) The experimental catalysts data for the maximum strength values and deformation energies used to support the findings of this study are currently under embargo while the research findings are commercialized. Requests for data, 12 months after publication of this article, will be considered by the corresponding author (Zhongren Wang; wzrvision@hbuas.edu.cn).

Conflicts of Interest

The authors declare that there are no conflicts of interest regarding the publication of this paper.

Acknowledgments

The authors gratefully acknowledge the use of the services and facilities of AVIC Hubei Aviation Precision Machinery Technology Co., Ltd., and Hubei Key Laboratory of Power System Design and Test for Electrical Vehicle. This research was funded by the Youth Project of Hubei Provincial Department of Education (No. Q20172603), Hubei Superior and Distinctive Discipline Group of Mechatronics and Automobiles (No. XKQ2018065), and Hubei Superior and Distinctive Discipline Group of Mechatronics and Automobiles (No. XKQ2018009).

References

[1] L. Xie, D. Palmer, F. Otto, Z. Wang, and Q. Jane Wang, "Effect of Surface Hardening Technique and Case Depth on Rolling Contact Fatigue Behavior of Alloy Steels," *Tribology Transactions*, vol. 58, no. 2, pp. 215–224, 2015.

[2] A. Emamian, "A Study on Wear Resistance, Hardness and Impact Behaviour of Carburized Fe-Based Powder Metallurgy Parts for Automotive Applications," *Materials Sciences and Applications*, vol. 03, no. 08, pp. 519–522, 2012.

[3] X. Y. Li, S. S. Li, and Q. L. Ceng, "Study on strength of carburized gear for mining gearbox based on dynamics," *Journal of China Coal Society*, vol. 36, no. 7, pp. 1227–1231, 2011.

[4] X. Y. Li, Q. X. Zhang, N. N. Wang, Q. L. Zeng, and K. Hidenori, "Meshing simulation and strength calculation of a carburized gear pair," *International Journal of Simulation Modelling*, vol. 16, no. 1, pp. 121–132, 2017.

[5] B. Jiang, X. Zheng, and L. Wu, "Estimate by fracture mechanics theory for rolling contact fatigue life and strength of case-hardened gear materials with computer," *Engineering Fracture Mechanics*, vol. 39, no. 5, pp. 867–874, 1991.

[6] Z. Chen and Y. Shao, "Mesh stiffness calculation of a spur gear pair with tooth profile modification and tooth root crack," *Mechanism and Machine Theory*, vol. 62, pp. 63–74, 2013.

[7] J.-Y. Tang and Y.-P. Liu, "Loaded multi-tooth contact analysis and calculation for contact stress of face-gear drive with spur involute pinion," *Journal of Central South University*, vol. 20, no. 2, pp. 354–362, 2013.

[8] F. O. Aramidea, S. A. Ibitoye, I. O. Oladele, and J. O. Borode, "Effects of carburization time and temperature on the mechanical properties of carburized mild steel, using activated carbon as carburizer," *Materials Research*, vol. 12, no. 4, pp. 483–487, 2009.

[9] J. John, K. Li, and H. Li, "Fatigue performance and residual stress of carburized gear steels Part I: Residual stress," *SAE International Journal of Materials and Manufacturing*, vol. 1, no. 1, pp. 718–724, 2009.

[10] N.-K. Kim and K.-Y. Bae, "Analysis of deformation in the carburizing-quenching heat treatment of helical gears made of SCM415H steel," *International Journal of Precision Engineering and Manufacturing*, vol. 16, no. 1, pp. 73–79, 2015.

[11] A. Sugianto, M. Narazaki, M. Kogawara, S. Y. Kim, and S. Kubota, "Distortion analysis of axial contraction of carburized-quenched helical gear," *Journal of Materials Engineering and Performance*, vol. 19, no. 2, pp. 194–206, 2010.

[12] A. R. Rajesh, G. Joseph, and K. A. Venugopal, "Design and Testing of Gears Operating between a Specified Center Distance Using Altered Tooth-sum Gearing (Z± Gearing)," *Journal of Mechanical Engineering and Automation*, vol. 6, no. 5A, pp. 102–108, 2016.

[13] K. Nojima, K. Ogata, M. Tanaka, R. Nishi, Y. Ono, and T. Koide, "Bending fatigue strength of case-carburized helical gears (In the case of large helix angles)," *Journal of Mechanical Science and Technology*, vol. 31, no. 12, pp. 5657–5663, 2017.

[14] G.-J. Du, Z.-Q. Yang, and X.-M. Liu, "Quenching process simulation of carburized cylindrical gear," *Gongcheng Lixue/Engineering Mechanics*, vol. 30, no. 1, pp. 407–412, 2013.

[15] Y. Zhang, W. Shi, L. Yang, Z. Gu, and Z. Li, "The Effect of Hardenability Variation on Phase Transformation of Spiral Bevel Gear in Quenching Process," *Journal of Materials Engineering and Performance*, vol. 25, no. 7, pp. 2727–2735, 2016.

[16] G. Deng, K. Inoue, N. Takatsu, and M. Kato, "Evaluation of the Strength of Carburized Spur Gear Teeth Based on Fracture Mechanics: (3rd Report, The Crack Growth in Carburized Gear)," *Transactions of The Japan Society of Mechanical Engineers Series C*, vol. 57, no. 535, pp. 909–913, 1991.

[17] K. Miyachika, B. D. I. Daing Mohamad Nafiz, T. Koide, B. W. N. Imadjiddin Helmi, and K. Ando, "Effects of rim and web thicknesses on root stresses of thin-rimmed helical gears," *Nihon Kikai Gakkai Ronbunshu, C Hen/Transactions of the Japan Society of Mechanical Engineers, Part C*, vol. 77, no. 775, pp. 597–603, 2011.

[18] C. Han, "The prediction research on fatigue failure under gear tooth surface," *Journal of Mechanical Transmission*, vol. 37, no. 8, pp. 1–5, 2011.

[19] H. Jiang, Y. Shao, and C. K. Mechefske, "Dynamic characteristics of helical gears under sliding friction with spalling defect," *Engineering Failure Analysis*, vol. 39, pp. 92–107, 2014.

[20] T. Xiang, L. Gu, and J. Xu, "The meshing angular velocity and tangential contact force simulation for logarithmic spiral bevel gear based on Hertz elastic contact theory," *Journal of Mechanical Science and Technology*, vol. 30, no. 8, pp. 3441–3452, 2016.

[21] I. Gonzalez-Perez, J. L. Iserte, and A. Fuentes, "Implementation of Hertz theory and validation of a finite element model for stress analysis of gear drives with localized bearing contact," *Mechanism and Machine Theory*, vol. 46, no. 6, pp. 765–783, 2011.

[22] P. Zhang, S. X. Li, and Z. F. Zhang, "General relationship between strength and hardness," *Materials Science and Engineering: A Structural Materials: Properties, Microstructure and Processing*, vol. 529, no. 1, pp. 62–73, 2011.

[23] M. F. Ashby and H. D. R. Jones, *Engineering Materials*, Pergamon, Oxford, UK, 1980.

[24] A. Saxena, A. Parey, and M. Chouksey, "Time varying mesh stiffness calculation of spur gear pair considering sliding friction and spalling defects," *Engineering Failure Analysis*, vol. 70, pp. 200–211, 2016.

[25] Y. Ding and N. F. Rieger, "Spalling formation mechanism for gears," *Wear*, vol. 254, no. 12, pp. 1307–1317, 2003.

[26] J. M. Gere and B. J. Goodno, *International Journal of Strength of Materials*, China machine press, Beijing, China, 2011.

[27] M. A. Muraro, F. Koda, U. Reisdorfer Jr., and C. H. da Silva, "The influence of contact stress distribution and specific film thickness on the wear of spur gears during pitting tests," *Journal of the Brazilian Society of Mechanical Sciences and Engineering*, vol. 34, no. 2, pp. 135–144, 2012.

[28] Z. Ren, S. Zhou, C. Li, and B. Wen, "Dynamic characteristics of multi-degrees of freedom system rotor-bearing system with coupling faults of rub-impact and crack," *Chinese Journal of Mechanical Engineering*, vol. 27, no. 4, pp. 785–792, 2014.

[29] H. Ma, X. Pang, R. Feng, R. Song, and B. Wen, "Fault features analysis of cracked gear considering the effects of the extended tooth contact," *Engineering Failure Analysis*, vol. 48, pp. 105–120, 2015.

[30] J. Shi, Z. S. Dai, Q. L. Deng, and B. Shen, "The available hardened depth of laser quenching of large module gears," *Journal of Mechanical Transmission*, vol. 30, no. 3, pp. 84–87, 2006.

[31] W. Xiao, Z. Liu, and Y. Yuan, "Design method of hardened depth for carburized gear," *Jinshu Rechuli/Heat Treatment of Metals*, vol. 39, no. 6, pp. 147–150, 2014.

[32] C. F. Yang, L. H. Chiu, and J. K. Wu, "Effects of carburization and hydrogenation on the impact toughness of AISI 4118 steel," *Surface and Coatings Technology*, vol. 73, no. 1-2, pp. 18–22, 1995.

[33] W. H. Yang, "A generalized von Mises criterion for yield and fracture," *Journal of Applied Mechanics*, vol. 47, no. 2, pp. 297–300, 1980.